


# Single and binary catalyst systems based on nickel and palladium in polymerization of ethylene

Mahsa Kimiaghali<sup>1</sup> | Hossein Nasr Isfahani<sup>1</sup> | Gholam Hossein Zohuri<sup>2</sup>  | Ali Keivanloo<sup>1</sup>

<sup>1</sup> Department of Chemistry, Shahrood University of Technology, PO Box 3619995161, Shahrood, Iran

<sup>2</sup> Department of Chemistry, Faculty of Sciences, Ferdowsi University of Mashhad, PO Box 91775, Mashhad, Iran

## Correspondence

Gholam Hossein Zohuri, Department of Chemistry, Faculty of Sciences, Ferdowsi University of Mashhad, PO Box 91775, Mashhad, Iran.  
Email: zohuri@um.ac.ir

The catalyst (*N,N*-bis(2,6-dibenzhydryl-4-ethoxyphenyl)butane-2,3-diimine) nickel dibromide, a late transition metal catalyst, was prepared and used in ethylene polymerization. The effects of reaction parameters such as polymerization temperature, co-catalyst to catalyst molar ratio and monomer pressure on the polymerization were investigated. The  $\alpha$ -diimine nickel-based catalyst was demonstrated to be thermally robust at a temperature as high as 90 °C. The highest activity of the catalyst (494 kg polyethylene (mol cat)<sup>-1</sup> h<sup>-1</sup>) was obtained at [Al]/[Ni] = 600:1, temperature of 90 °C and pressure of 5 bar. In addition, the performance of a binary catalyst using nickel- and palladium-based complexes was compared with that of the corresponding individual catalytic systems in ethylene polymerization. In a study of the catalyst systems, the average molecular weight and molecular weight distribution for the binary polymerization were between those for the individual catalytic polymerizations; however, the binary catalyst activity was lower than that of the two individual ones. The obtained polyethylenes had high molecular weights in the region of 10<sup>5</sup> g mol<sup>-1</sup>. Gel permeation chromatography analysis showed a narrow molecular weight distribution of 1.44 for the nickel-based catalyst and 1.61 for the binary catalyst system. The branching density of the polyethylenes generated using the binary catalytic system (30 branches/1000 C) was lower than that generated using the nickel-based catalyst (51/1000 C). X-ray diffraction study of the polymer chains showed higher crystallinity with lower branching of the polymer obtained. Also Fourier transform infrared spectra confirmed that all obtained polymers were low-density polyethylene.

## KEYWORDS

binary catalyst polymerization, catalytic polymerization, late transition metals, LDPE, polyethylene

## 1 | INTRODUCTION

Polyethylene materials and polymerization of  $\alpha$ -olefins play essential roles in industrial production.<sup>[1]</sup> Initial reports by Brookhart and co-workers revealed that complexes of nickel and palladium bearing sterically hindered  $\alpha$ -diimine ligands could generate high-molecular-weight polymers with high catalytic activity in

ethylene polymerization.<sup>[2,3]</sup> The properties and reactions of metal complexes are highly dependent on the selection of supporting ligand(s),<sup>[4–7]</sup> and this selection is one of the keys to successful coordination chemistry. Late transition metal catalysts based on bulky bis(imine)ligands usually depend on the structures of ligands and *ortho*-position groups on the aryl rings that showed very interesting behaviours in olefin polymerization.<sup>[8]</sup> Nickel- and

palladium-based catalysts generally exhibit poor thermal stability at elevated temperatures that are required for industrial application.<sup>[9]</sup> This is due to increasing *N*-aryl rotations from perpendicular to square-planar coordination plane at higher temperatures. This not only decreases steric hindrance at the axial sites thus accelerating chain transfer reaction, but also leads to the potential decomposition arising from C—H activation of the metal centre to the ligand.<sup>[10]</sup> Improvements in  $\alpha$ -diimine catalyst thermal stability have been reported through various modification of ligand backbone and *N*-aryl substituents.<sup>[11–16]</sup> For instance, catalysts bearing camphorquinone-derived ligands have shown moderate stability up to 80 °C.<sup>[17]</sup> Recently, benzhydryl-derived ligand substructures were investigated.<sup>[18–22]</sup> We also reported a catalyst that demonstrated good thermal stability up to 80 °C producing polyethylene molecular weight of  $8.1 \times 10^4 \text{ g mol}^{-1}$ .<sup>[23]</sup> The spherical morphology of the catalyst and polyethylene with moderate branching density of 40.5/1000 C and melting point in the range 66–111 °C were the most significant reported results. Moreover, these values were higher than those reported by Chen and co-workers for similar catalysts bearing Me, OMe, Cl and CF<sub>3</sub> groups.<sup>[24]</sup>

The bulk of an *ortho*-position group expectedly inhibits the *N*-aryl rotation of an  $\alpha$ -diimine ligand because of repulsive interaction, thus enhancing thermal stability. In order to better understand the effect of prepared  $\alpha$ -diimine ligands and to further explore the potential of these catalysts, the analogous nickel(II) complex was synthesized and used for ethylene polymerization. The effects of reaction parameters such as polymerization temperature, co-catalyst to catalyst molar ratio and monomer pressure were investigated.

Chain-walking mechanism of nickel- and palladium-based complexes allows them to produce polymers with a broad spectrum of branching topologies, ranging from relatively linear to hyperbranched or dendritic.<sup>[25]</sup> The control of polymer topology through chain walking mechanism in the polymerization process offers great

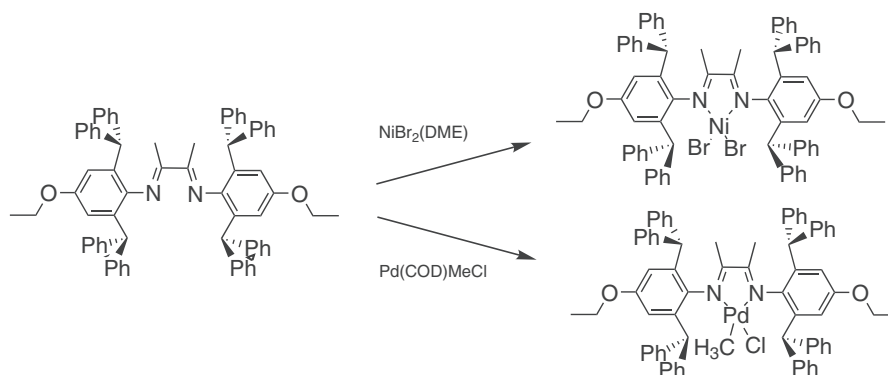
opportunities in the development of novel polymeric materials. In most cases, polyethylene properties are controlled by changing its molecular weight, molecular weight distribution and polymer chain branching. One of the main strategies used for the improvement of polyolefin catalysts, which is still being investigated at the laboratory scale, is the use of a combination of different types of catalysts during polymerization. Catalyst alloys, hybrid catalysts and multi-catalyst systems are commonly used in this respect.<sup>[26–31]</sup> In these systems, each of the catalysts produces polymers with different properties, and therefore the final polymer is a blend of two or more kinds of polymers. To achieve new architectures and characteristic properties, a mixture of late transition metal complexes was used for ethylene polymerization. This type of polymerization has been studied in a few cases.<sup>[25,32,33]</sup>

To study the performance of a binary catalyst system, nickel- and palladium-based complexes with ligands containing  $\alpha$ -diimine framework with dibenzhydryl moieties were synthesized as shown in Scheme 1. The performance of the binary system in ethylene polymerization was compared with that of corresponding individual catalytic systems.

## 2 | EXPERIMENTAL

### 2.1 | Materials

All manipulation of air- and water-sensitive compounds were conducted under inert atmosphere (nitrogen/argon) using standard Schlenk and glovebox techniques. Argon, nitrogen and ethylene gas were purified by passing through activated columns of silica gel, KOH and 4 Å/13X types of molecular sieves. All solvents were dried prior to use. Toluene was dried over calcium hydride and distilled over sodium/benzophenone. Dichloromethane and *n*-hexane also were purified over calcium hydride and diethyl ether was purified over sodium/



**SCHEME 1** Synthesis route of the catalysts

benzophenone. 4-Ethoxyaniline (purity of 99.9%, Merck) was distilled. Diacetyl (97%) and diphenylmethanol (98%) were supplied by Merck. Triisobutylaluminium (purity of 93%) was supplied by Sigma-Aldrich (Germany) which was used in the synthesis of modified methylaluminoxane (MMAO) according to the literature.<sup>[34]</sup> 1,2-Dimethoxyethane nickel(II) bromide ((DME)NiBr<sub>2</sub>), chloro(1,5-cyclooctadiene)methylpalladium and sodium tetrakis(3,5-bis(trifluoromethyl)phenyl)borate (NaBAF) were purchased from Sigma-Aldrich.

## 2.2 | Instrumentation

<sup>1</sup>H NMR and <sup>13</sup>C NMR spectra of organic compounds were recorded with a Bruker Avance III (300 MHz). High-temperature NMR analysis of polyethylene was performed with a Bruker Avance 400 (400 MHz). Elemental analysis was performed with a Thermo Finnigan EA1112 CHN elemental analyser. Fourier transform infrared (FT-IR) spectra were obtained using an Avatar 370 FT-IR spectrometer. Mass spectra were recorded using a Varian CH-7A spectrometer. Thermogravimetric analysis (TGA; PerkinElmer TGA-7) and differential scanning calorimetry (DSC; Mettler Toledo DSC 822e) with a scan rate of 10 °C min<sup>-1</sup> were used for characterization of polyethylene. Scanning electron microscopy (SEM) images were obtained using a LEO VP 1450 instrument. High-temperature gel permeation chromatography (GPC) was performed using 3-chlorobenzene solvent (PL-GPC 220). X-ray diffraction (XRD) analysis was carried out with a Unisantis XMD-300.

## 2.3 | Catalyst preparation

The syntheses of *N,N'*-bis(2,6-dibenzhydryl-4-ethoxyphenyl)butane-2,3-diimine as a ligand and corresponding (*N,N'*-bis(2,6-dibenzhydryl-4-ethoxy phenyl)butane-2,3-diimine)palladium methyl chloride complex have been reported in our recent work.<sup>[23]</sup>

### 2.3.1 | Synthesis of (*N,N*-bis(2,6-dibenzhydryl-4-ethoxy phenyl)butane-2,3-diimine)nickel dibromide

To (DME)NiBr<sub>2</sub> (0.023 g, 0.076 mmol) in a Schlenk flask under an inert atmosphere, a solution of the prepared ligand (0.076 g, 0.076 mmol) in dichloromethane (5 ml) was added dropwise. After stirring of the mixture for 24 h at room temperature, the solvent was partially evaporated under reduced pressure and the remaining solution was diluted in diethyl ether. The red solid was isolated by centrifugation and dried under high vacuum. This precatalyst was used in the polymerization process

without further purification. Anal. Calcd for C<sub>72</sub>H<sub>64</sub>Br<sub>2</sub>N<sub>2</sub>NiO<sub>2</sub> (%): C, 71.60; H, 5.34; N, 2.32. Found (%): C, 72.12; H 5.73; N, 1.88. FT-IR (KBr, cm<sup>-1</sup>): 1599 (C=N), 449 (Ni—N).

## 2.4 | General procedure for catalysed ethylene polymerization

Ethylene polymerization reactions using the prepared nickel catalyst and 1:1 mixture of the nickel and palladium complexes were carried out under various polymerization conditions. The high-pressure process was performed in a 1 l Buchi bmd 300-type stainless steel reactor while that at low pressure was carried out in a two-neck flask equipped with magnetic stirrer and ethylene inlet. The appropriate toluene solvent and NaBAF (if needed) were introduced in to the reactor under an inert atmosphere. The reactor was repeatedly evacuated and refilled with argon and then with ethylene gas. Desired temperature was set and MMAO as co-catalyst was added. The complex(es) dissolved in 2 ml of dichloromethane were introduced into the reactor. Immediately the reactor was pressurized and the solution was stirred for 30 min. The polymerization was terminated by venting unreacted monomer and adding 10 vol% HCl-methanol solution. The polymer was washed with an excess of methanol and dried at room temperature.

## 3 | RESULTS AND DISCUSSION

### 3.1 | Catalyst

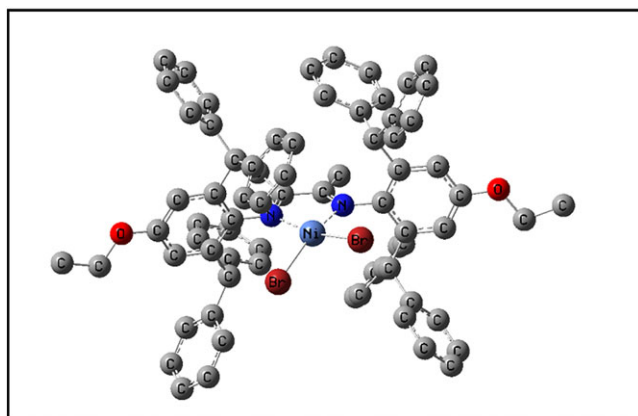
The general structures of the catalysts are depicted in Scheme 1. The ligand was prepared by conventional Schiff base condensation.<sup>[23]</sup> The palladium complex structure has been reported in our previous work.<sup>[23]</sup> The nickel-based catalyst was formed by addition of the ligand to (DME)NiBr<sub>2</sub>. The reaction was completed in 24 h. The crystalline red complex was obtained at room temperature by diffusion of diethyl ether into dichloromethane solution of the corresponding complex. The structure of the product was confirmed using elemental and FT-IR analyses. The nickel complex is very sensitive to moisture.

Gaussian software<sup>[35]</sup> was applied to build up the structure and calculate the structural parameters of the complex. Quantum chemical calculations were performed with the density functional theory method using B3LYP function and LanL2DZ basis set. Results are gathered in Table 1, giving optimized structures, bond distances, bond angles, dipole moments, charge and total energy of the complex. The optimized structure of the complex (Figure 1) shows the very large hindering and electronic effects as obtained for the palladium complex.<sup>[23]</sup> The

**TABLE 1** Calculated parameters for the nickel complex<sup>a</sup>

Parameter	Result	Parameter	Result
Ni–Br <sub>1</sub>	2.39	Ni–C <sub>6</sub>	3.93
Ni–Br <sub>2</sub>	2.38	Br <sub>1</sub> –Ni–Br <sub>2</sub>	90.17
Ni–N <sub>1</sub>	1.98	Ni–N <sub>1</sub> –C <sub>1</sub>	113.39
Ni–N <sub>2</sub>	1.97	Ni–N <sub>2</sub> –C <sub>2</sub>	113.37
C <sub>1</sub> =N <sub>1</sub>	1.31	N <sub>2</sub> –Ni–N <sub>1</sub>	82.57
C <sub>2</sub> =N <sub>2</sub>	1.31	Dipole moment (D)	10.56
N <sub>1</sub> –C <sub>3</sub>	1.46	Band gap	0.083
N <sub>2</sub> –C <sub>4</sub>	1.46	Total energy	–3237.4 a.u.
C <sub>2</sub> –C <sub>1</sub>	1.49	Charge(Mulliken)	–0.051
Ni–C <sub>5</sub>	3.79		

<sup>a</sup>Selected bond distances (Å), bonding angle and plane angle (°). Br<sub>1</sub>: bromine atom in front; Br<sub>2</sub>: bromine atom behind; N<sub>1</sub>: nitrogen atom connected to right-hand side aryl ring; N<sub>2</sub>: nitrogen atom connected to left-hand side aryl ring; C<sub>1</sub>: carbon of C–CH<sub>3</sub> bond in right-hand side of molecule; C<sub>2</sub>: carbon of C–CH<sub>3</sub> bond in left-hand side of molecule; C<sub>3</sub>: aryl ring carbon connected to N<sub>1</sub>; C<sub>4</sub>: aryl ring carbon connected to N<sub>2</sub>; C<sub>5</sub>: carbon atom on *ortho* position of major aryl ring in right-hand side of complex; C<sub>6</sub>: carbon atom on *ortho* position of major aryl ring in left-hand side of complex.

**FIGURE 1** Optimized structure of the nickel complex catalyst (hydrogen atoms omitted for clarity)

relationship between activity and net charge of the central metal atom indicated that a complex with higher charge has higher activity, which is different from that reported for early transition metal systems.<sup>[36]</sup> The nickel complex showed higher net charge of the central metal atom than the palladium complex,<sup>[23]</sup> and, based on this, had higher polymerization activity.

### 3.2 | Ethylene polymerization using nickel-based catalyst

The results for ethylene polymerization catalysed by the nickel complex are listed in Table 2. The ethylene polymerization was carried out under various conditions.

The effect of co-catalyst/catalyst molar ratio (MMAO as co-catalyst) on the polymerization behaviour was investigated. The highest activity was obtained at [Al]:[Ni] = 600:1. It is conceivable that two bulky groups at *ortho* position prevent the catalyst from coordination to the co-catalyst leading to easier ethylene insertion to the active centres. On the other hand, the propagation reaction occurs only when the complex formed by the cationic catalyst and MMAO is dissociated.<sup>[37]</sup> Higher molar ratios of Al/Ni enhance chain transfer from nickel active species on to aluminium and then form polyethylenes with lower molecular weights.<sup>[38]</sup>

To evaluate the thermal stability of the nickel-based catalyst and to overcome the limitation associated with elevated reaction temperatures, polymerization was performed at 40, 68, 80 and 90 °C (Table 2). The prepared catalyst showed high thermal stability as evidenced by the highest activity at 90 °C. Study of the effect of polymerization temperature and kinetics of polymerization on the catalyst behaviour revealed that the polymerization temperature can enhance the catalyst efficiency through increasing the kinetic energy of the monomer molecules which facilitates transfer of ethylene to the catalytic active centres and also increasing alkylation of metal centres.<sup>[25]</sup> The activity of the catalyst was increased by increasing the monomer pressure up to 3.5 bar; however, further increase of the monomer pressure led to a decrease of the catalyst activity. This behaviour is mainly due to higher concentration of the monomer close to the active centre which has an effect on diffusion, site activation and also propagation rate.<sup>[39,40]</sup> A nonlinear relationship between monomer pressure and activity was previously reported.<sup>[41–43]</sup> However, higher pressure can cause a reverse effect on the catalyst activity especially by formation of latent sites or dormant sites.<sup>[42]</sup>

### 3.3 | Ethylene polymerization using mixture of nickel- and palladium-based catalysts

To determine the appropriate co-catalyst, experiments were carried out using a mixture of the nickel and palladium complexes in the presence of various amounts of both MMAO and NaBAF co-catalysts. According to our previous work,<sup>[23]</sup> 2 eq. of NaBAF was used for the palladium-based catalyst. MMAO was used for activation of the nickel-based catalyst. The results for ethylene polymerization using the mixture of nickel and palladium complexes are summarized in Table 3. In general, high activities were achieved with a mixture of 2 eq. of NaBAF and 600:1 molar ratio of [MMAO]:[Ni].

**TABLE 2** Result for ethylene polymerization with nickel-based catalyst<sup>a</sup>

Entry	Co-cat. [al]/[Ni]	T (°C)	P (atm)	Activity <sup>b</sup>	$M_v (\times 10^4 \text{ g mol}^{-1})$	$T_m (\text{°C})^c$	Crystallinity (%)
1	300	80	1.5	135.04	—	—	—
2	600	80	1.5	206.67	6.68	d	d
3	800	80	1.5	152.46	—	—	—
4	1500	80	1.5	111.80	—	—	—
5	1800	80	1.5	—	—	—	—
6	600	40	1.5	96.32	2.81	d	d
7	600	68	1.5	128.26	4.39	51.45	11.65
8	600	90	1.5	352.84	17.91	28.12	20.46
9	600	90	1	5.81	—	—	—
*10	600	90	3.5	494.16	28.08	120	0.53
*11	600	90	5.0	38.24	0.52	37.10	6.80

<sup>a</sup>Polymerization conditions: 4.13  $\mu\text{mol}$  of nickel catalyst, polymerization time = 30 min, 38 ml (\*200 ml) of toluene, 2 ml of  $\text{CH}_2\text{Cl}_2$ . Some oily products were obtained in all tests.

<sup>b</sup>Activity: kg of polyethylene (mol cat)<sup>−1</sup> h<sup>−1</sup>.

<sup>c</sup>Melting temperature determined using DSC (second heating).

<sup>d</sup>Completely amorphous polymer.

**TABLE 3** Result for ethylene polymerization with mixture of nickel- and palladium-based catalysts<sup>a</sup>

Entry	Co-cat [al]/[Ni]	Co-cat NaBAF	T (°C)	P (atm)	Activity <sup>b</sup>	$M_v (\times 10^4 \text{ g mol}^{-1})$	$T_m (\text{°C})^c$	Crystallinity (%)
1	300	2	60	1.5	23.00	—	—	—
2	1300	2	60	1.5	23.66	—	—	—
3	1700	2	60	1.5	50.00	—	—	—
4	—	2 + 2	60	1.5	43.32	—	—	—
5	600	2	60	1.5	113.32	11.76	80.43	5.21
6	600	2	60	3.0	453.29	45.04	95.21	15.97
7	600	2	60	5.0	346.63	37.91	95.34	13.27

<sup>a</sup>Polymerization conditions: 3  $\mu\text{mol}$  of palladium-based catalyst and 3  $\mu\text{mol}$  of nickel-based catalyst, polymerization time = 30 min, 38 ml (\*200 ml) of toluene, 2 ml of  $\text{CH}_2\text{Cl}_2$ . Some oily products were obtained in all of the tests.

<sup>b</sup>Activity: kg of polyethylene (mol cat)<sup>−1</sup> h<sup>−1</sup>.

The effect of temperature on catalyst behaviour was investigated. The optimum temperature was 40 °C for the palladium-based catalyst and 90 °C for the nickel-based one. Ethylene polymerization using the mixture of the two catalysts was conducted with the average of these polymerization temperatures considering the optimum temperature for both catalysts (60 °C).

The influence of monomer pressure on behaviour of the mixture of nickel- and palladium-based catalysts was studied in the range 1.5–5 bar, while the co-catalyst ratio and polymerization temperature were kept constant at  $[\text{MMAO}]:[\text{Ni}] = 600:1$  and 2 eq. of NaBAF. According to Table 3 (entries 5–7), the highest activity was obtained at a monomer pressure of 3 bar. However, further increasing of the monomer pressure to 5 bar led

to a small decrease in catalyst activity. This phenomenon is attributed to the cooperative effect between the catalyst centres in the binary catalyst system. According to literature reports, the rate of chain growth is independent of olefin concentration for the palladium catalyst.<sup>[22,44]</sup> However, for the nickel-based catalyst, as discussed in Section 3.2, the activity decreases at higher monomer pressure.

### 3.4 | Morphological study

Polymers obtained using the palladium-based catalyst were almost spherical with some links among the spherical parts as has been reported.<sup>[23]</sup> Morphological studies were carried out for the nickel-based catalyst,



and polyethylene obtained using both the nickel-based catalyst and mixture of nickel and palladium-based catalysts. No regular morphology was observed for the nickel-based catalyst using SEM (Figure 2). The SEM images in Figure 3 correspond to polymers obtained using the nickel-based catalyst (Table 2, entry 8). It can be observed from Figure 3 that the polyethylene particles are quite irregular. The polymer obtained using the mixture of the catalysts is also not a regular form (Figure 3). The bulky polymer particles are composed of many small porous particles like the polymers obtained using the nickel-based catalyst.

### 3.5 | Polymer molecular weight

The viscosity-average molecular weight ( $M_v$ ) of some polymer samples was determined using an Ubbelohde viscometer. Higher  $M_v$  of the produced polyethylene at different pressure and temperature was in the region of

$10^5 \text{ g mol}^{-1}$  (Tables 2 and 3).  $M_v$  increases with increasing polymerization temperature. Such behaviour is due to the ease of entry of monomers into the reaction centre and supplying energy to carry out propagation reactions as the temperature of the reaction increases.<sup>[45]</sup>

The molecular weight of some polyethylene samples was determined using GPC analysis in trichlorobenzene. These results and some for the palladium-based catalysis previously reported<sup>[23]</sup> are presented in Table 4 and Figure 4 for comparison. A polymer having high number-average molecular weight ( $M_n$ ) was produced using the nickel-based catalyst. The mix of the two catalysts afforded polymers with lower average molecular weight than the nickel-based catalyst but higher than the palladium-based catalyst. Moreover, GPC curves showed narrow molecular weight distribution and polydispersity index (PDI) of 1.44 for the polymer obtained using the nickel-based catalyst, while there was a peak along with a shoulder for the sample produced using the palladium-based catalyst and a wider shoulder for the sample produced using the mixture of catalysts. The shoulder in the GPC peak can be attributed to a difference in molecular weight of polymer chains that is a result of different rates of monomer insertion and chain transfer ( $K_{ins}/K_{ct}$ ) of each catalyst centre.<sup>[32,37]</sup> Therefore using the mix of catalysts showed greater difference in distribution of product molecular weight. The resulting products have the properties of mixtures of polymers obtained under the action of the corresponding individual catalytic systems.

### 3.6 | Polymer thermal properties

Thermal stability is a very significant property for polymers. It is often the limiting factor in polymer processing and applications. The thermal stability of polyethylene samples were investigated using TGA under nitrogen atmosphere. The thermogravimetric and differential thermogravimetric curves are shown in Figures 5 and 6. The TGA curves do not show any significant change in the onset of degradation temperature for the three polymer samples. Differential thermogravimetric curves clarify that degradation occurred mainly in the range 350–520 °C for the nickel-based catalyst polyethylene sample and 400–500 °C for the palladium-based catalyst polymer sample, but it is in the range 400–520 °C for the polymer obtained using the binary catalytic system. Polyethylene obtained using the mix of nickel- and palladium-based catalysts has higher thermal stability than that obtained using each of the single catalysts. It is decomposed in several steps more than the nickel- or palladium-based catalyst polymer samples because of greater difference in distribution of its molecular weight.<sup>[46]</sup>

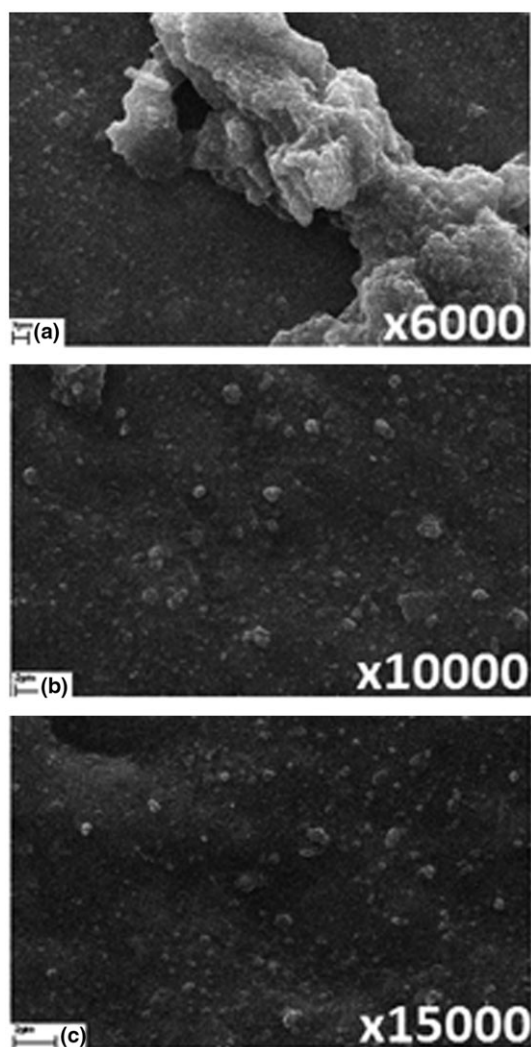
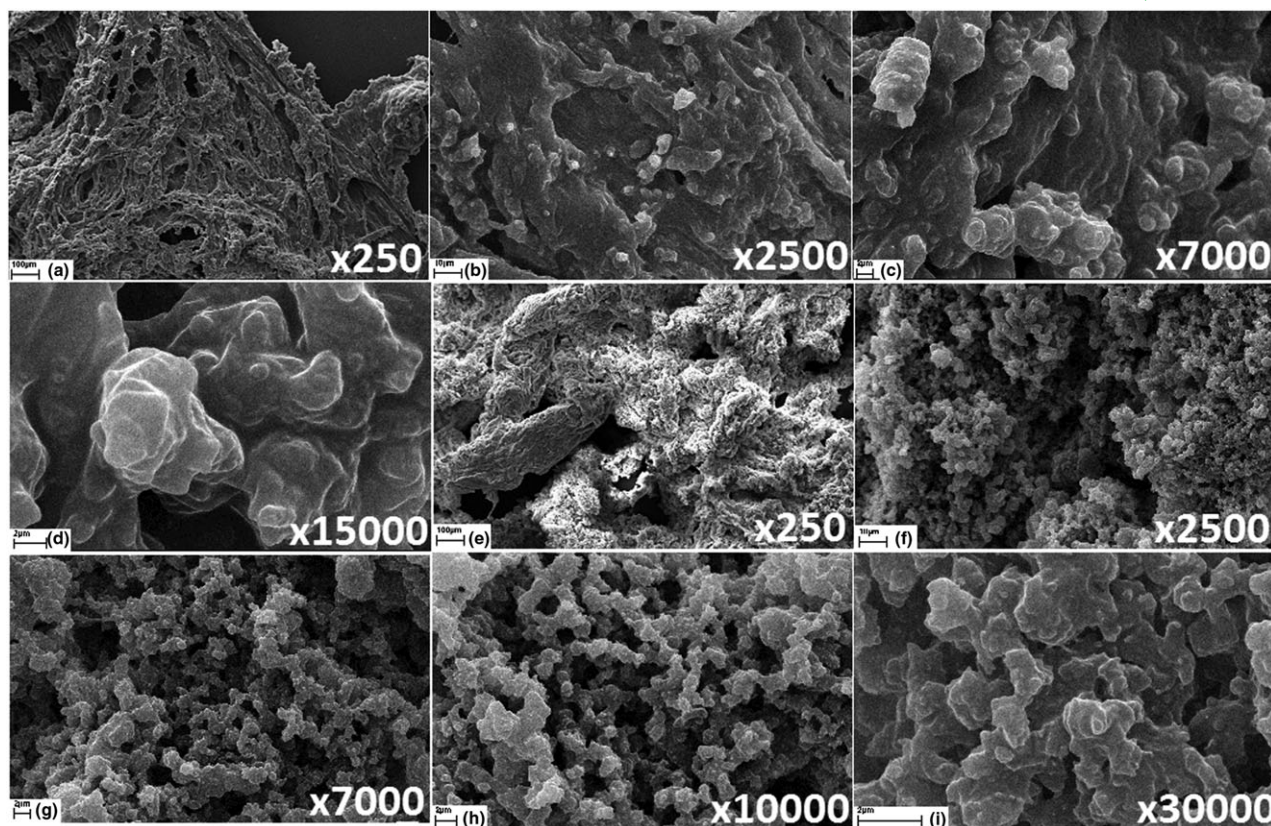


FIGURE 2 SEM micrographs of nickel-based catalyst



**FIGURE 3** SEM images of polyethylene: (a–d) entry 8 of Table 2; (e–i) entry 6 of Table 3

**TABLE 4** Properties of resulting polyethylene

Sample	Catalyst	$T_p$	Activity <sup>a</sup>	$M_n (\times 10^4 \text{ g mol}^{-1})^b$	$M_w (\times 10^4 \text{ g mol}^{-1})^b$	PDI <sup>b</sup>	Branch/1000 C <sup>c</sup>
Previous work <sup>[23]</sup>	Pd(II)	40	168	4.40	8.09	1.83	40.5
Entry 8, Table 2	Ni(II)	90	353	17.3	25.03	1.44	51.3
Entry 5, Table 3	Ni(II), Pd(II)	60	113	6.62	10.67	1.61	30.2

<sup>a</sup>Activity: kg of polyethylene (mol cat)<sup>−1</sup> h<sup>−1</sup>.

<sup>b</sup>Determined by GPC.

<sup>c</sup>Determined by <sup>1</sup>H NMR.

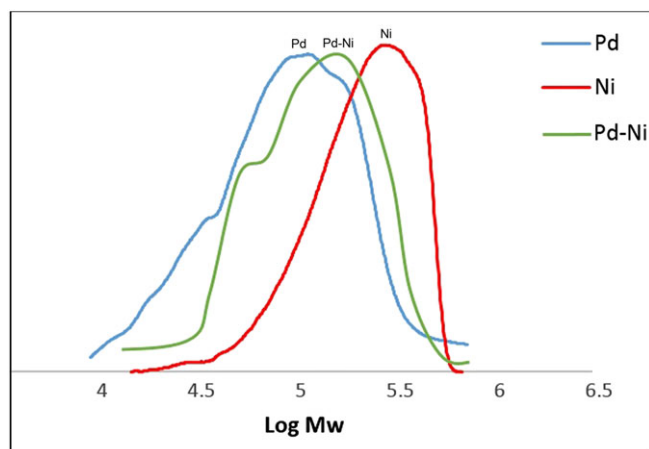


**FIGURE 4** GPC curves of polyethylene (three samples of Table 4)

Melting point and crystallinity values obtained from second heating of DSC thermograms are listed in Tables 2 and 3. The crystallinity of polyethylene, which significantly affects the properties of the polymer, is quite sensitive to the concentration of its branches.<sup>[47]</sup> The polymers produced using the nickel-based catalyst have low melting point due to much more branches and weaker intermolecular forces that was confirmed using NMR spectroscopy. Discussion of NMR analyses of polymers can be found in Section 3.7. Moreover, the thermograms indicated that the crystallinity of polyethylene increased with increasing polymerization temperature. It can be suggested that the increasing kinetic energy of the monomers due to rising temperature can facilitate transfer of

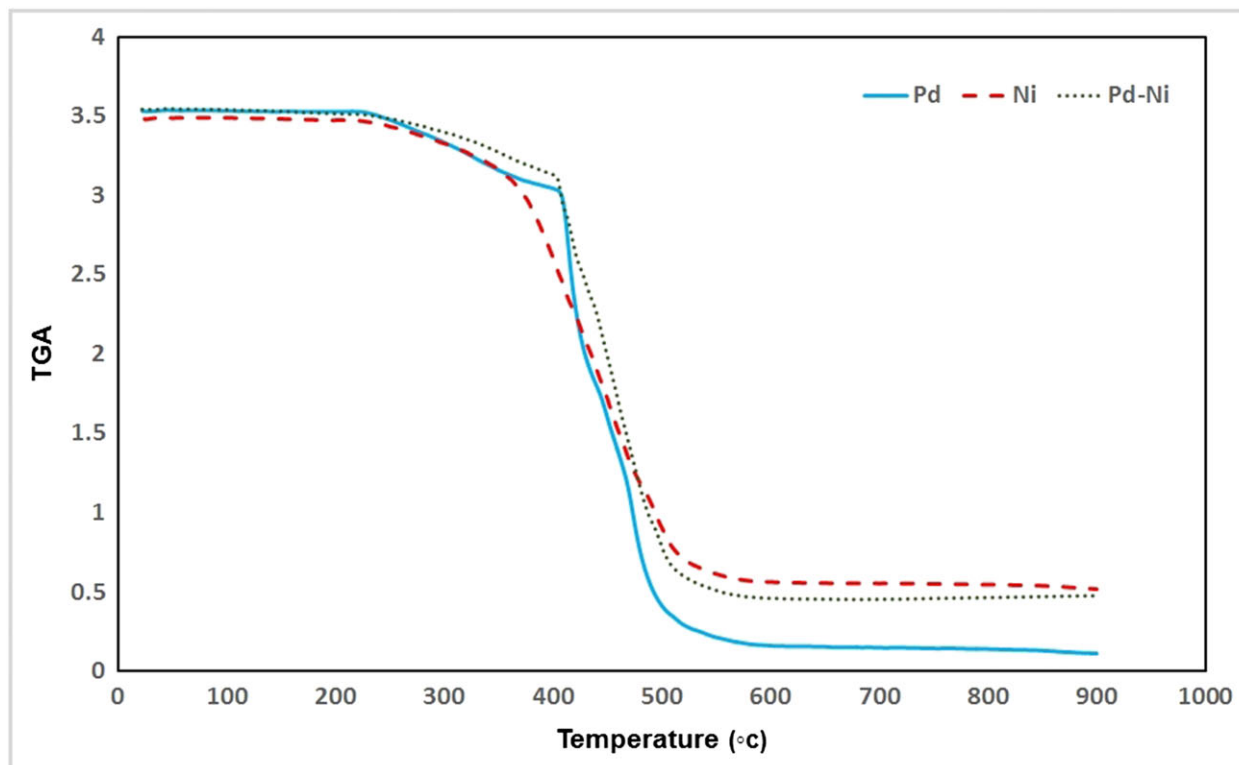


**FIGURE 5** TGA curves of polyethylene produced using different catalysts

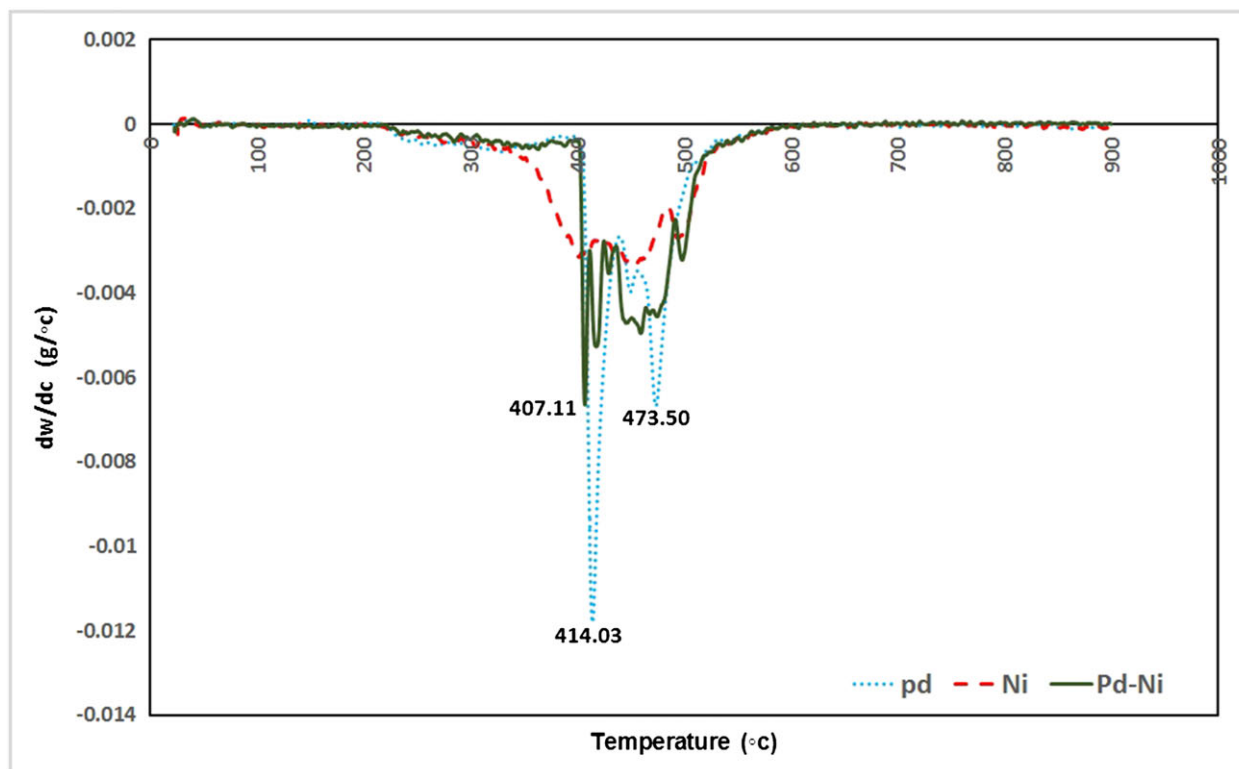


**FIGURE 6** Differential thermogravimetric curves of polyethylene produced using different catalysts

monomer to the catalytic active centres. The polyethylene obtained using the mixture of nickel- and palladium-based catalysts generally showed higher  $T_m$  values than

the polymer obtained using the nickel-based catalytic system, and these values are in the range of those previously reported for the palladium-based catalyst.<sup>[23]</sup>



### 3.7 | Microstructure study

Two polyethylene samples (Table 2, entry 8; Table 3, entry 5) were characterized using high-temperature  $^1\text{H}$  NMR and  $^{13}\text{C}$  NMR spectroscopy. The NMR spectra were obtained at 50 °C in  $\text{CDCl}_3$ . The  $^{13}\text{C}$  NMR spectra of the polymers, assignments and the microstructure determination of the branched polyethylenes are presented in

Figures 7 and 8. The  $^{13}\text{C}$  NMR spectra were interpreted according to the literature.<sup>[48–50]</sup> Branches are named as  $x\text{B}_n$ , where  $n$  is the length of the branch and  $x$  is the carbon number starting from the methyl group as '1'. For branch point carbons, 'br' is used instead of  $x$  and the methylenes of the backbone are labelled with Greek letters. For paired branches lower-case subscripts are used (pee: 1,3-paired ethyl ethyl branches, peq: 1,3-paired ethyl

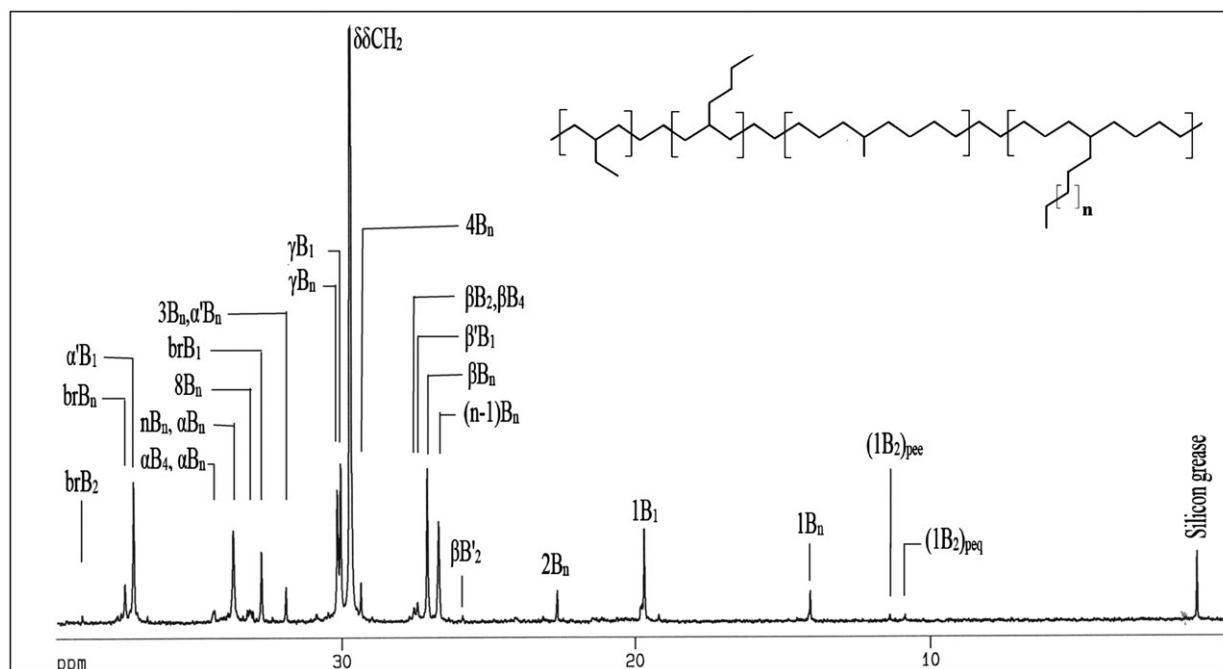


**FIGURE 7**  $^{13}\text{C}$  NMR spectrum of polymer from Table 2, entry 8 ( $\text{CDCl}_3$ , 50 °C)

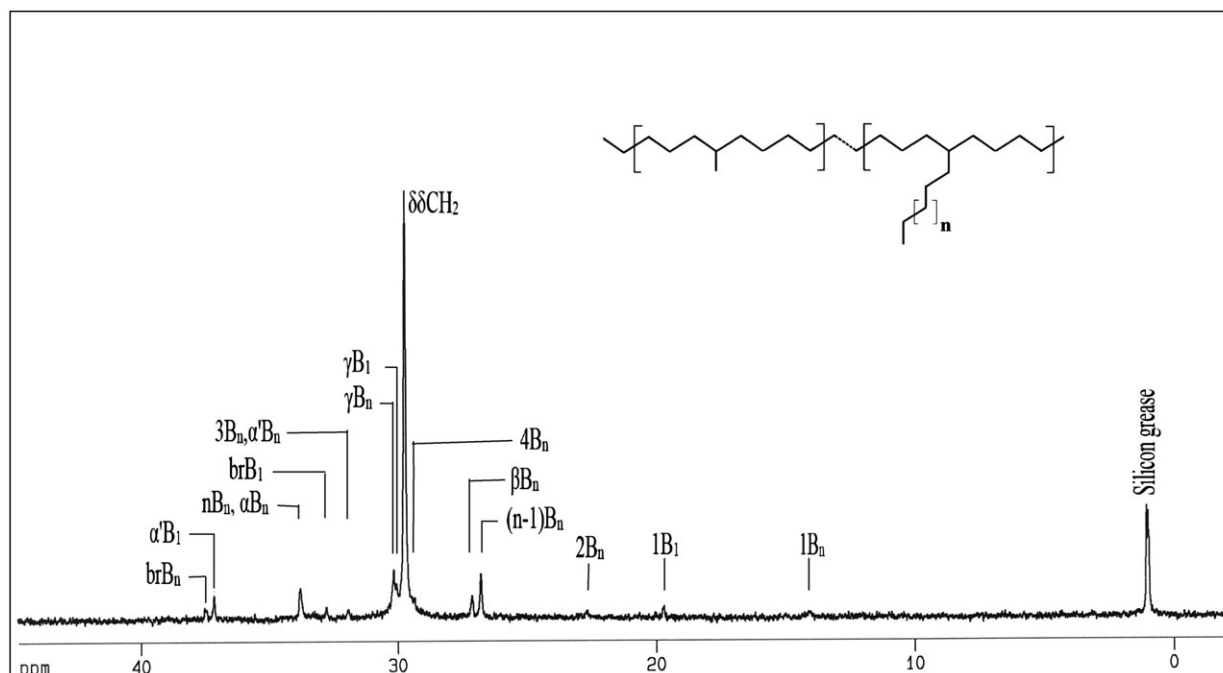


**FIGURE 8**  $^{13}\text{C}$  NMR spectrum of polymer from Table 3, entry 6 ( $\text{CDCl}_3$ , 50 °C)

ethyl branches attached to quaternary carbons).<sup>[50]</sup>  $^1\text{H}$  NMR spectroscopy was used to determine overall branching in the polymers.<sup>[51]</sup> Results are reported in Table 4. Both samples have moderate branches, individually indicating 51 branches per 1000 carbons in the nickel-based catalyst polymer sample and 30 branches per 1000 carbons in the mix of nickel- and palladium-based catalyst polymer sample. These are lower than branching of samples produced using each catalyst alone.<sup>[23]</sup> The degree of polymer branching can be modulated via polymerization conditions and catalyst structures. As  $^{13}\text{C}$  NMR spectra illustrate, the nickel-based catalyst produced a polymer with methyl, ethyl, butyl and long-chain branches. But the mixture of the catalysts produced a polymer with methyl and long-chain branching as has been reported for the palladium-based catalyst.<sup>[23]</sup> These results suggested that the chain walking process can be controlled in olefin polymerization.<sup>[40]</sup> Long and co-workers described the synthesis of a similar  $\alpha$ -diimine nickel complex with H,  $\text{CH}_3$  and acenaphthyl groups, generating moderately branched (63–75 branches per 1000 carbons) polyethylene.<sup>[17,52]</sup> Also recently Chen and co-workers reported studies of  $\alpha$ -diimine nickel complexes with Cl and  $\text{OCH}_3$  groups in ethylene polymerization. The branching density of the polyethylene generated using those complexes (34–62 branches/1000 carbons) is much lower than that of polyethylene produced using classic

Brookhart catalyst (*ca* 100 branches/1000 carbons).<sup>[15]</sup> All these benzhydryl-based nickel and palladium catalysts are very slow chain walking polymerization catalysts. The chain walking process can be suppressed in  $\alpha$ -diimine system through ligand modifications.<sup>[40]</sup>

The FT-IR spectra of the polyethylene products confirmed that all samples are low-density polyethylene (LDPE).<sup>[53]</sup> The region  $1300\text{--}1400\text{ cm}^{-1}$  displayed three bands assignable to  $\text{CH}_2$  and  $\text{CH}_3$  groups. Bands at  $1377\text{ cm}^{-1}$  are assigned to  $\text{CH}_3$  symmetric deformation and bands in the regions  $1366$  and  $1351\text{ cm}^{-1}$  correspond to wagging deformation. The LDPE microstructure has long-chain branches in the structure which prevents molecules from packing closely together and the irregular packing causes low crystallinity content and low melting point, as was confirmed from the results discussed in Section 3.6 for the thermal properties of produced polymers.<sup>[54,55]</sup>

The XRD patterns of three polyethylene samples of Table 4 are presented in Figure 9. For the polymer obtained using the binary catalytic system, the characteristic peak shows an increase in the sharpness, indicating an increase in the degree of crystallinity which can be as a result of strong interactions between different polymer chain interfaces.<sup>[56,57]</sup> There is a broadening and reduction in intensity of peaks for the corresponding individual catalytic systems, indicative of altered amorphous and

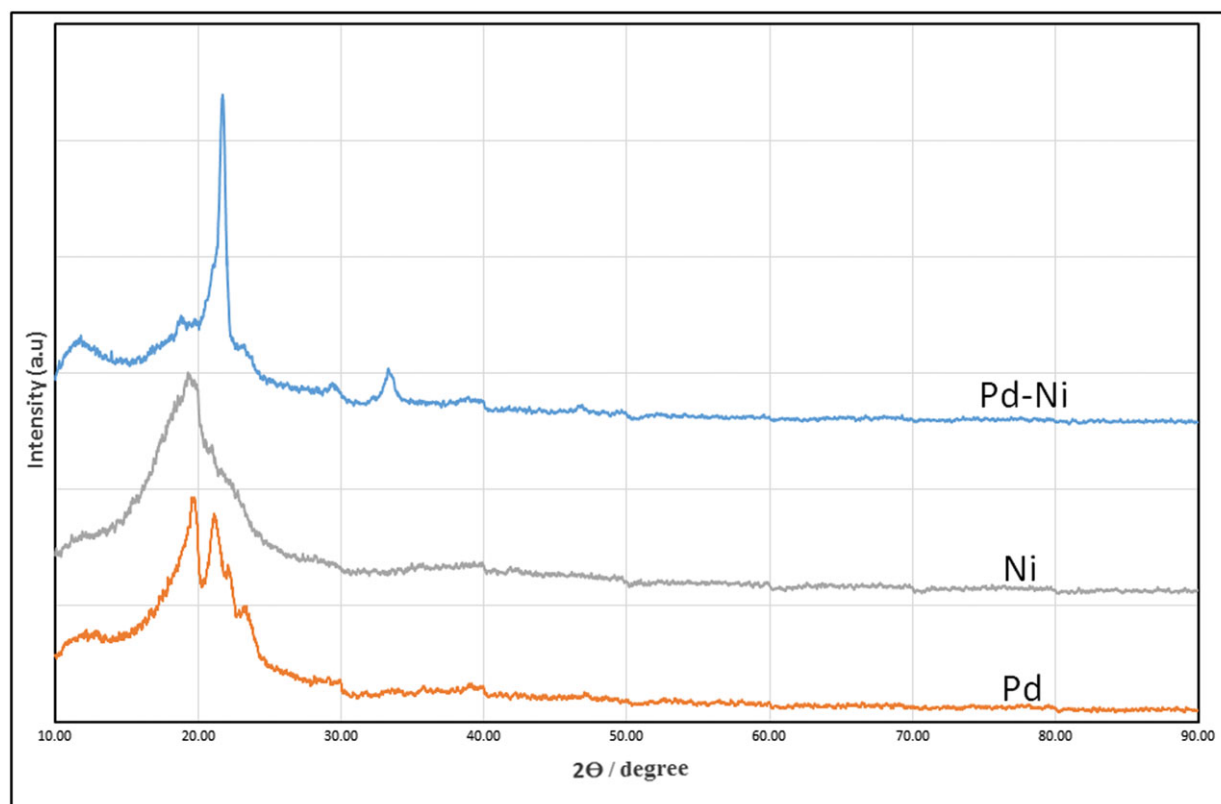


**FIGURE 9** XRD patterns of polyethylene powder obtained using various catalytic systems

crystalline phases. This means that using the binary catalytic system caused an enhancement in the crystallinity of the polymer. Such behaviour could be a result of reducing the number of branches from 51 in 1000 carbons in the polymer obtained using the single catalyst. However, for the binary catalyst system the branching was 30 in 1000 carbon atoms in the polymer chain.

## 4 | CONCLUSIONS

The prepared nickel  $\alpha$ -diimine catalyst with benzhydryl-derived ligand framework and ethoxy group in the *para* position of *N*-aryl group was an active catalyst in ethylene polymerization. This catalyst activated with MMAO exhibited high activity up to 494.16 kg polyethylene (mol cat)<sup>-1</sup> h<sup>-1</sup>. To obtain the optimum conditions in the polymerization, effects of Al/Ni molar ratio, temperature and pressure of monomer on the polymerization were studied. Thermal stability of the catalyst was evaluated up to 90 °C, and no catalyst decomposition was seen at that temperature during the polymerization period. The produced polyethylene sample exhibited narrow polydispersity (PDI = 1.44) and high molecular weight ( $1.73 \times 10^5$  g mol<sup>-1</sup>) and 51 branches/1000 C. The nickel-based catalyst showed higher activity than the palladium-based analogue. This observation was confirmed by higher net charge of the central nickel atom than palladium charge as determined from quantum chemical calculations. Furthermore, a mixture of the palladium and nickel  $\alpha$ -diimine complexes was employed in ethylene polymerization using both NaBAF and MMAO as co-catalysts. Molecular weight and polydispersity of polyethylene obtained using the binary catalyst system were between the values for the corresponding individual catalytic systems. The ethylene polymerization activity of the nickel- and palladium-based catalysts was higher than that of mixed complexes. When NaBAF (2 eq./Pd) and MMAO(Al/Ni 600:1 molar ratio) were used as co-catalysts, the productivity of the binary catalyst system improved, but it produced polyethylene with less degree of branching (30 branches/1000 C) than using each of the individual catalysts. The results revealed that the activity of each complex is predominantly suppressed due to selective activation of the metallic centre in the binary catalyst system; however, thermal stability of the products was improved. Polymers obtained using both the binary and individual catalytic systems were LDPE as confirmed from FT-IR spectra. The binary catalytic system improved the crystallinity of the resulting polymer, which could be due to a reduction of the branching from 51 to 30 in 1000 carbon atoms of the polymer chain obtained from single and binary catalyst systems, respectively.

## ORCID

Gholam Hossein Zohuri  <http://orcid.org/0000-0003-2380-8363>

## REFERENCES

- [1] D. B. Malpass, *Introduction to Industrial Polyethylene: Properties, Catalysts, and Processes*, Vol. 45, John Wiley, Hoboken, NJ **2010**.
- [2] L. K. Johnson, C. M. Killian, M. Brookhart, *J. Am. Chem. Soc.* **1995**, *117*, 6414.
- [3] C. M. Killian, D. J. Tempel, L. K. Johnson, M. Brookhart, *J. Am. Chem. Soc.* **1996**, *118*, 11664.
- [4] S. Ahmadjo, S. Damavandi, G. H. Zohuri, A. Farhadipour, Z. Etemadinia, *J. Organometal. Chem.* **2017**, *835*, 43.
- [5] S. Damavandi, G. H. Zohuri, R. Sandaroos, S. Ahmadjo, *Polym. Sci. Ser. B* **2017**, *59*, 1.
- [6] W. Tao, S. Akita, R. Nakano, S. Ito, Y. Hoshimoto, S. Ogoshi, K. Nozaki, *Chem. Commun.* **2017**, *53*, 2630.
- [7] T. Liang, C. Chen, *Organometallics* **2017**, *36*, 2338.
- [8] M. Khoshsefat, N. Beheshti, G. H. Zohuri, S. Ahmadjo, S. Soleimanzadegan, *Polym. Sci. Ser. B* **2016**, *58*, 487.
- [9] T. Xie, K. B. McAuley, J. C. Hsu, D. W. Bacon, *Ind. Eng. Chem. Res.* **1994**, *33*, 449.
- [10] L. Zhong, G. Li, G. Liang, H. Gao, Q. Wu, *Macromolecules* **2017**, *50*, 2675.
- [11] D. Meinhard, M. Wegner, G. Kipiani, A. Hearley, P. Reuter, S. Fischer, O. Marti, B. Rieger, *J. Am. Chem. Soc.* **2007**, *129*, 9182.
- [12] A. S. Ionkin, W. J. Marshall, *Organometallics* **2004**, *23*, 3276.
- [13] J. Liu, D. Chen, H. Wu, Z. Xiao, H. Gao, F. Zhu, Q. Wu, *Macromolecules* **2014**, *47*, 3325.
- [14] H. Hu, L. Zhang, H. Gao, F. Zhu, Q. Wu, *Chem. Eur. J.* **2014**, *20*, 3225.
- [15] L. Guo, S. Dai, C. Chen, *Polymers* **2016**, *8*, 37.
- [16] H. Gao, H. Hu, F. Zhu, Q. Wu, *Chem. Commun.* **2012**, *48*, 3312.
- [17] J. L. Rhinehart, L. A. Brown, B. K. Long, *J. Am. Chem. Soc.* **2013**, *135*, 16316.
- [18] E. Yue, Q. Xing, L. Zhang, Q. Shi, X. P. Cao, L. Wang, C. Redshaw, W. H. Sun, *Dalton Trans.* **2014**, *43*, 3339.
- [19] E. Yue, L. Zhang, Q. Xing, X. P. Cao, X. Hao, C. Redshaw, W. H. Sun, *Dalton Trans.* **2014**, *43*, 423.
- [20] S. Kong, C. Y. Guo, W. Yang, L. Wang, W. H. Sun, R. Glaser, *J. Organometal. Chem.* **2013**, *725*, 37.
- [21] J. Lai, X. Hou, Y. Liu, C. Redshaw, W. H. Sun, *J. Organometal. Chem.* **2012**, *702*, 52.
- [22] Z. Zhou, X. Hao, C. Redshaw, L. Chen, W. H. Sun, *Catal. Sci. Technol.* **2012**, *2*, 1340.
- [23] M. Kimiaghali, H. N. Isfahani, G. H. Zohuri, A. Keivanloo, *Inorg. Chim. Acta* **2017**, *464*, 99.
- [24] S. Dai, X. Sui, C. Chen, *Angew. Chem. Int. Ed.* **2015**, *54*, 9948.
- [25] H. PourTaghi Zahed, G. H. Zohuri, *Polym. Bull.* **2013**, *70*, 1769.

- [26] B. Jiang, Y. Yang, L. Du, J. Wang, Y. Yang, S. Stapf, *Ind. Eng. Chem. Res.* **2013**, 52, 2501.
- [27] Y. Zhao, L. Wang, H. Yu, G. Jing, C. Li, Y. Chen, M. Saleem, *J. Polym. Res.* **2014**, 21, 470.
- [28] I. Sedov, L. Russiyan, L. Blinova, G. Davydova, E. Knerel'man, L. Vasil'eva, Y. I. Zlobinsky, *J. Polym. Res.* **2014**, 21, 583.
- [29] J. P. McInnis, M. Delferro, T. J. Marks, *Acc. Chem. Res.* **2014**, 47, 2545.
- [30] S. Ahmadjo, S. Dehghani, G. H. Zohuri, G. R. Nejabat, H. Jafarian, M. Ahmadi, S. M. M. Mortazavi, *Macromol. React. Eng.* **2015**, 9, 8.
- [31] S. M. M. Mortazavi, H. Jafarian, M. Ahmadi, S. Ahmadjo, *J. Therm. Anal. Calorim.* **2016**, 123, 1469.
- [32] I. V. Sedov, P. E. Matkovskiy, *Russian Chem. Rev.* **2012**, 81, 239.
- [33] T. Sun, Q. Wang, Z. Fan, *Polymer* **2010**, 51, 3091.
- [34] S. A. Sangokoya, Google Patents EP 0463555B1, **1996**.
- [35] M. Frisch, G. Trucks, H. Schlegel, G. Scuseria, M. Robb, J. Cheeseman, G. Scalmani, V. Barone, B. Mennucci, G. Petersson, Gaussian Inc., Wallingford, CT, **2009**.
- [36] G. H. Zohuri, S. M. Seyedi, R. Sandaroos, S. Damavandi, A. Mohammadi, *Catal. Lett.* **2010**, 140, 160.
- [37] S. Damavandi, N. Samadieh, S. Ahmadjo, Z. Etemadinia, G. H. Zohuri, *Eur. Polym. J.* **2015**, 64, 118.
- [38] L. Fan, S. Du, C. Y. Guo, X. Hao, W. H. Sun, *J. Polym. Sci. A: Polym. Chem.* **2015**, 53, 1369.
- [39] F. AlObaidi, Z. Ye, S. Zhu, *Polymer* **2004**, 45, 6823.
- [40] L. Guo, S. Dai, X. Sui, C. Chen, *ACS Catal.* **2015**, 6, 428.
- [41] H. Arabi, M. Beheshti, M. Yousefi, N. G. Hamedani, M. Ghafelebashi, *Polym. Bull.* **2013**, 70, 2765.
- [42] L. C. Simon, C. P. Williams, J. B. Soares, R. F. de Souza, *J. Mol. Catal. A* **2001**, 165, 55.
- [43] S. Ahmadjo, S. Damavandi, G. H. Zohuri, A. Farhadipour, N. Samadieh, Z. Etemadinia, *Polym. Bull.* **2017**, 74, 3819.
- [44] D. J. Tempel, L. K. Johnson, R. L. Huff, P. S. White, M. Brookhart, *J. Am. Chem. Soc.* **2000**, 122, 6686.
- [45] G. H. Zohuri, S. Damavandi, R. Sandaroos, S. Ahmadjo, *Polym. Bull.* **2011**, 66, 1051.
- [46] S. C. Moldoveanu, *Analytical Pyrolysis of Synthetic Organic Polymers*, Vol. 25, Elsevier **2005**.
- [47] M. Jung, Y. Lee, S. Kwak, H. Park, B. Kim, S. Kim, K. H. Lee, H. S. Cho, K. Y. Hwang, *Anal. Chem.* **2016**, 88, 1516.
- [48] G. B. Galland, R. F. de Souza, R. S. Mauler, F. F. Nunes, *Macromolecules* **1999**, 32, 1620.
- [49] G. B. Galland, R. Quijada, R. Rojas, G. Bazan, Z. J. Komon, *Macromolecules* **2002**, 35, 339.
- [50] T. Usami, S. Takayama, *Macromolecules* **1984**, 17, 1756.
- [51] A. C. Gottfried, M. Brookhart, *Macromolecules* **2003**, 36, 3085.
- [52] J. L. Rhinehart, N. E. Mitchell, B. K. Long, *ACS Catal.* **2014**, 4, 2501.
- [53] J. Gulmine, P. Janissek, H. Heise, L. Akcelrud, *Polym. Test.* **2002**, 21, 557.
- [54] A. A. Klyosov, *Wood-Plastic Composites*, John Wiley, New York **2007**.
- [55] C. Vasile, M. Pascu, *Practical Guide to Polyethylene*, iSmithers Rapra Publishing, London **2005**.
- [56] N. Senso, S. Khaubunsongserm, B. Jongsomjit, P. Praserttham, *Molecules* **2010**, 15, 9323.
- [57] Z. Mo, H. Zhang, *J. Macromol. Sci. C* **1995**, 35, 555.

**How to cite this article:** Kimiaghali M, Isfahani HN, Zohuri GH, Keivanloo A. Single and binary catalyst systems based on nickel and palladium in polymerization of ethylene. *Appl Organometal Chem.* 2017;e4153. <https://doi.org/10.1002/aoc.4153>